Aceh Int. J. Sci. Technol., 3(1): 27-36
April 2014
doi: 10.13170/AIJST.0301.03

Aceh International Journal of Science and Technology

ISSN: 2088-9860
Journal homepage: http://jurnal.unsyiah.ac.id/aijst

Surface Energy Balance in Jakarta and Neighboring Regions As Simulated Using Fifth Mesoscale Model (MM5)

Yopi Ilhamsyah
Meteorological Division, Department of Marine Sciences, Syiah Kuala University, Banda Aceh 23111, Indonesia. Corresponding email: y.ilhamsyah@gmail.com

Received : February 7, 2014
Accepted : April 26, 2014

Abstract – The objective of the present research was to assess the surface energy balance particularly in terms of the computed surface energy and radiation balance and the development of boundary layer over Jakarta and Neighboring Regions (JNR) by means of numerical model of fifth generation of Mesoscale Model (MM5). The MM5 with four domains of 9 kilometers in spatial resolution presenting the outermost and the innermost of JNR is utilized. The research focuses on the third and fourth domains covering the entire JNR. The description between radiation and energy balance at the surface is obtained from the model. The result showed that energy balance is higher in the city area during daytime. Meanwhile, energy components, e.g., surface sensible and latent heat flux showed that at the sea and in the city areas were higher than other areas. Moreover, ground flux showed eastern region was higher than others. In general, radiation and energy balance was higher in the daytime and lower in the nighttime for all regions. The calculation of Bowen Ratio, the ratio of surface sensible and latent heat fluxes, was also higher in the city area, reflecting the dominations of urban and built-up land in the region. Meanwhile, Bowen Ratio in the rural area dominated by irrigated cropland was lower. It is consistent with changes of land cover properties, e.g. albedo, soil moisture, and thermal characteristics. In addition, the boundary layer is also higher in the city. Meanwhile western region dominated by suburban showed higher boundary layer instead of eastern region.
Keywords: MM5; Energy components; Land cover properties

Introduction

The portion of incoming solar radiation received on the earth mostly determines the formation of weather and climate. Global averages of incoming and outgoing radiation is recognized to have equal portion. When the incoming radiation, classified in short-wave frequency, entering the atmosphere, large portion of radiation reach the earth and experience surface absorption and reflection, only small portion is scattered and reflected back by clouds and suspended particles (i.e., aerosol) in the atmosphere (Trenberth, 2014). The incoming Short-Wave Radiation (SWR) is transferred into heat (e.g., sensible and latent heat) and energy processes (e.g., potential and kinetic energy) before it is re-radiated to the atmosphere in the form of Long-Wave Radiation (LWR). The exchange of energy into various forms generates a variety of weather and associated phenomena in the atmosphere. As a result, Surface Energy Balance (SEB) may effect to the changes of weather and climate in time.

The physical characteristics of the earth and atmosphere are governed by contributions of incoming SWR and outgoing LWR. The incoming solar radiation intensity at the top of the

atmosphere as well as its transmission through the atmosphere controls SWR received at the surface. The amount of outgoing radiation depends on surface reflection properties characterized by albedo, which has variation in number. In addition, higher radiation at the surface is affected by greenhouse gas emission, so-called the incoming LWR. The radiation from the earth is emitted back to the atmosphere, later known as the outgoing LWR. Following the condition, the emission rate is influenced by surface temperature and emissivity based on Stefan-Boltzman law. The conservation of energy between air and land develop the relationship between net radiation and turbulence fluxes, i.e., SEB. In the same manner, SEB can be derived by combining the incoming SWR and outgoing LWR (Holtslag and Steeneveld, 2008).

Jakarta, the metropolitan city, and neighboring regions, e.g., Depok, Tangerang, and Bekasi are believed to have variation in surface energy. These are resulted from differences of land properties which may further lead to weather variation over the region. Sofyan *et al.* (2007), Tokairin *et al.* (2009), and Ilhamsyah (2012) found that the weather over JNR can vary between north-south and west-east regions. The north-south regions cover the Java Sea to northern coast of Jakarta, low-lying Jakarta city, and hilly to mountainous areas in Depok and Bogor. Meanwhile, the west-east parts include suburban and industrial zones in Tangerang and residential areas also center for agriculture and fisheries activity in Bekasi and Depok. The west-east has relatively flat topography compared to the north-south regions. Thus, the condition may develop variation in SEB over the whole regions.

The research of SEB is often carried out theoretically combined with the availability of meteorological observation data or satellite images, such as Su (2002) who developed SEB system by combining satellite data and meteorological variables. Similarly, Xin and Liu (2010) used remote sensing technique to measure surface heat flux and Rouse *et al.* (2003) conducted a field measurement to observe SEB over certain region. However, such kind of research certainly require significant amount of cost since it is related to the expenses for instrumentation including any other supports, calibration and maintenance cost as well as accommodation and labor cost. In order to cope with the problem, it is necessary to develop a model in which the output is able to provide a good description of SEB over study areas. Numerical model such as MM5, firstly developed by Dudhia (1993), can be applied to deal with the challenge. Despite the fact that the model is created to study a meso-scale weather condition, but the spatial resolution can be adjusted up to 1-2 km, as done by Aquilina *et al.* (2005), Dagestad *et al.* (2006) and Sindosi *et al.* (2012). Besides, the model as early development purpose is a dynamic model that can be used for weather forecasting, thus, it bring benefit not only in reconstructing the past or current weather condition but also in presenting future weather condition, including SEB. The investigation of SEB by using MM5 has been carried out such as Oncley dan Dudhi (1995) and Grossman-Clarke *et al.* (2005). Hence, by referring to the success of MM5 to estimate SEB over various areas and fact that energy balance over JNR is not a subject of exploration yet motivate the present research, this paper attempt to assess SEB particularly in terms of the computed of surface energy and radiation balance and the development of boundary layer over JNR using numerical model MM5. This study will benefit to find the significances as well as differences of SEB between the city and west-east region of JNR.

Materials and Methods

The research is carried out by performing MM5, a three-dimensional non-hydrostatic sigma-pressure level where terrain profile is included in the model. The model is governed by fundamental atmospheric dynamic equation of motion (Pielke, 2002). There are 4 domains representing the outer and innermost of JNR (Figure 1). Outer domains, the first and second domain, cover the entire West Java and Southwest Java with spatial resolutions of 9 km. Meanwhile, inner domains depict the third and fourth domain covering JNR. These two inner domains also have spatial resolutions (Δx dan Δy) of 9 kilometers Besides, 35 levels ranging from

1000-100 hPa containing 15 levels of high resolution near the surface is also utilized in the model. The model also implements the following physical parameterization:

- Medium Range Forecast Planetary Boundary Layer (MRF PBL) scheme. The scheme is chosen to determine better surface heat flux computation. The scheme is also used by Durante and de Paus (2006), Deng and Stauffer (2006), and Ruiz-Arias *et al.* (2008) in their MM5 experiment study,
- Grell Cumulus scheme in the first and second domain,
- Cloud atmospheric radiation scheme.

Additionally, the initial boundary conditions applied in the model are as follows:

- 30-seconds (0.925 km) of USGS terrain height,
- 30-seconds (0.925 km) of modified 24 global categories of USGS land cover,
- 0.5° x 0.5° of meteorological data retrieved from ECMWF such as zonal and meridional wind, temperature, relative humidity, geopotential height, etc.

Modified land cover is used since the initial data released by USGS does not represent the current condition of JNR's land cover (Figure 2a). The inaccuracies of land cover data is also identified by some studies, such as Brazel *et al.* (2003) and Grossman-Clarke *et al.* (2005, 2007). Thus, land cover data need to be improved before the model is run. The land cover is modified manually by setting the appropriate land cover in the initial condition that can mimic the present condition of JNR captured from Google Earth. As a result, the fourth domain has approached the actual urban areas and other land cover condition in JNR (Figure 2b). The land cover improvement is also done in the third domain. Since land cover has changed, it also has an impact on changes of land properties, i.e., albedo, soil moisture, thermal and surface roughness. Therefore, the model is expected to give a good description in producing SEB over JNR. The research focuses on the third and fourth domains covering a whole JNR. Furthermore, the strategies of the research are:

- to apply the modified land cover into the initial boundary condition,
- to run the model,
- to visualize and to evaluate the model by comparing with the observation data, and
- to assess the SEB over JNR.

The simulation last for 5 days on August 04-08, 2004 during dry season. This date is selected to see how high the diurnal variation of energy in this period where precipitation is less, and also to compare with Sofyan *et al.* (2005). The model needs to be warmed-up for the first day of simulation to adjust all required physical parameterization and initial condition. Therefore, analysis focuses on the second day of simulation. Short simulation is done to avoid the initial value problem that arises in numerical weather prediction since most of the model is designed for short to medium ranges of weather prediction.

In general, the net radiation of incoming and outgoing radiation at the earth surface is calculated by using the following partition of SWR and LWR:

$$R_n = S\downarrow + S\uparrow + L\downarrow + L\uparrow, \quad (1)$$

where: R_n = surface net radiation.
$S\downarrow$ = incoming SWR.
$S\uparrow$ = outgoing SWR.
$L\downarrow$ = incoming LWR.
$L\uparrow$ = outgoing LWR.

By other means, SEB can also be simply written as:

$$R_n = H + L_vE + G. \qquad (2)$$

Where:
R_n = net radiation (Wm^{-2}).
L_vE = latent heat flux (Wm^{-2}), this flux help to cool the earth surface due to evaporation.
H = sensible heat flux (Wm^{-2}).
G = ground heat flux (Wm^{-2}). All SEB components as mentioned above are derived from MM5 simulation.

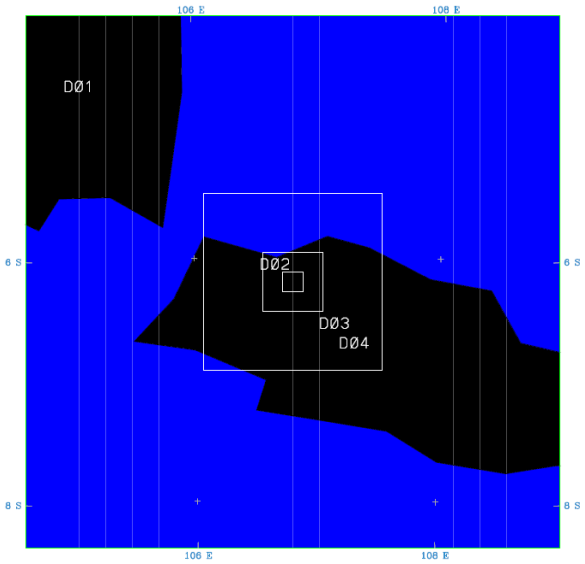

Figure 1. Domain of MM5 model.

Results and Discussion

The result shows that the simulated surface temperature is under-expected even though the urban areas have been expanded. The simulated temperature was taken at one point in domain 4 which was exactly located at airport weather station in the western region. The model is not well-coincided with the measured weather data. The temperature differences reach 6.4 K in the afternoon. However, a similar pattern describing the rise and the fall of temperature where it reachs a certain value of maximum and minimum temperature during day and nighttime between the model and field observation show a good comparison. The model is also consistent with temperature simulated by Sofyan *et al.* (2005, Figure 3). Based on the result, the paper confidently describes the simulated SEB over JNR

The incoming SWR at the surface is shown in figure 4a. All incoming radiation at the surface over JNR in the daytime received the same amount of energy. On August 05 and 06, maximum energy in the daytime reached 950 Wm^{-2} in all surface land cover. On August 08, the amount of energy received in the city was slightly higher than other regions. The variation of SEB is strongly affected by local weather condition which might be influenced by cloud cover or other conditions that directly absorb and reduce the amount of energy received at the surface.

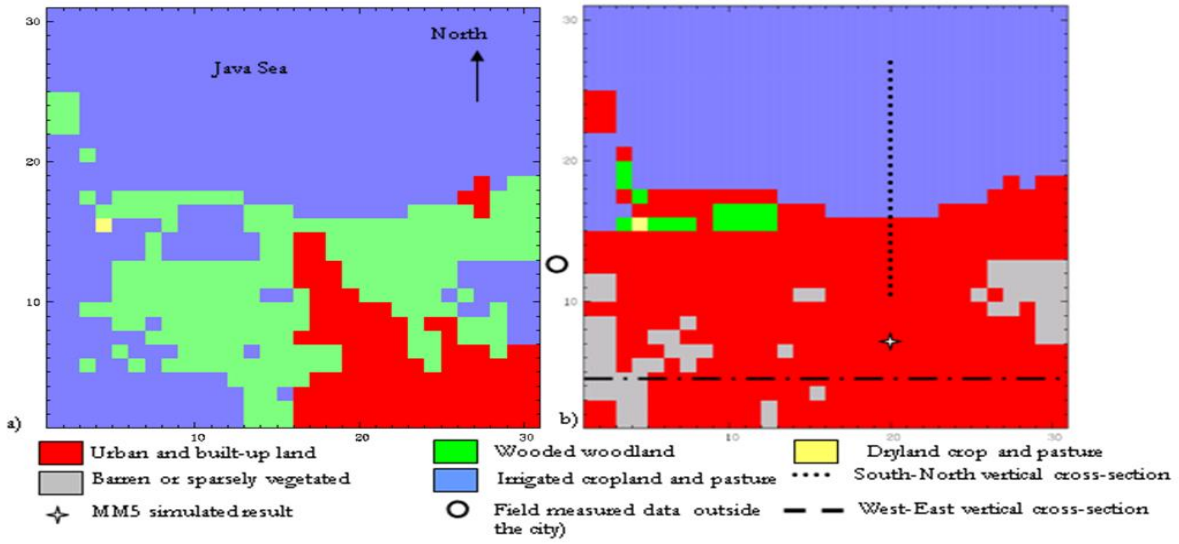

Figure 2. Land cover of MM5 model for the fourth domain, (a) standard-release USGS land cover and (b) modified USGS land cover.

The outgoing SWR from the surface is shown in figure 4b. It is noted that higher radiation occurs at the sea area in five days simulation except on August 7 where radiation in the region was the lowest. It might be due to local weather characteristics where cloud cover could inhibit the penetration of radiation to the surface causing low radiation that is emitted back to the atmosphere. Meanwhile, the outgoing radiation released from the eastern region was higher than the city area and western region. The condition is influenced by physical characteristics of land cover, e.g., albedo, soil moisture, emissivity, surface roughness and thermal inertia. Urban areas in city with building materials such as asphalt and concrete absorb more heat so that only little heat is reflected back to the atmosphere. The situation looks similar to the western region. The difference condition was found in the eastern region where farmland, vegetation, and water body still dominant, which have an impact on the higher reflected radiation. Albedo for such areas may reach 15-20%. Meanwhile, albedo of 05-15 % is found on land cover dominated by built-up areas, asphalt, and parks. Albedo of 05-80 % occurs at the sea leading to higher outgoing SWR from the region (Stull, 2000).

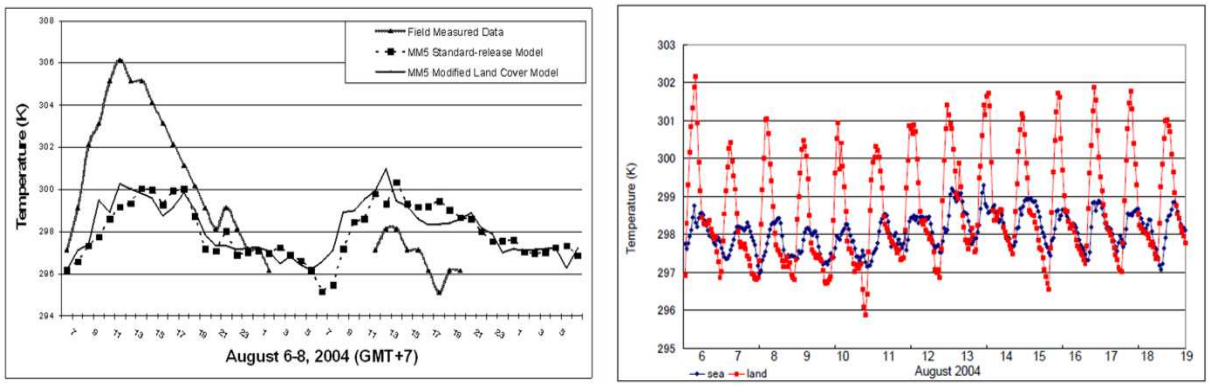

Figure 3. (a) Simulated temperature and its comparison to the observation and (b) Sofyan *et al.* (2005).

The incoming and outgoing LWR are shown in Figure 4c and 4d. The outgoing LWR originates from energy emitted from the earth surface. In the city area, the outgoing LWR was lower than western and eastern regions. Meanwhile, higher LWR was found in the western instead of the eastern region. The outgoing radiation is then absorbed by greenhouse gases in the atmosphere and is radiated back to the earth surface. The condition leads the earth temperature to become warmer. In figure 4c, the incoming LWR is higher in the city and western region reaching 460 Wm^{-2} of energy. Meanwhile, the eastern region receives as much as 450 Wm^{-2} of energy. On August 07, the amount of energy is less than 450 Wm^{-2}. The eastern region also shows significant diurnal variation as illustrated on August 07 and 08. The condition is caused by the absence of energy stored in land cover that can be reradiated back to the atmosphere in the nighttime. Difference conditions were observed in the western region, city area, and also at the sea where building material serves as storage as well as emitter particularly in the nighttime. The same thing applies at the sea where we know that during daytime, heat is absorbed slowly by the sea and during nighttime, heat is released back causing nighttime temperature over the sea is warmer than surrounding areas (Figure 4d).

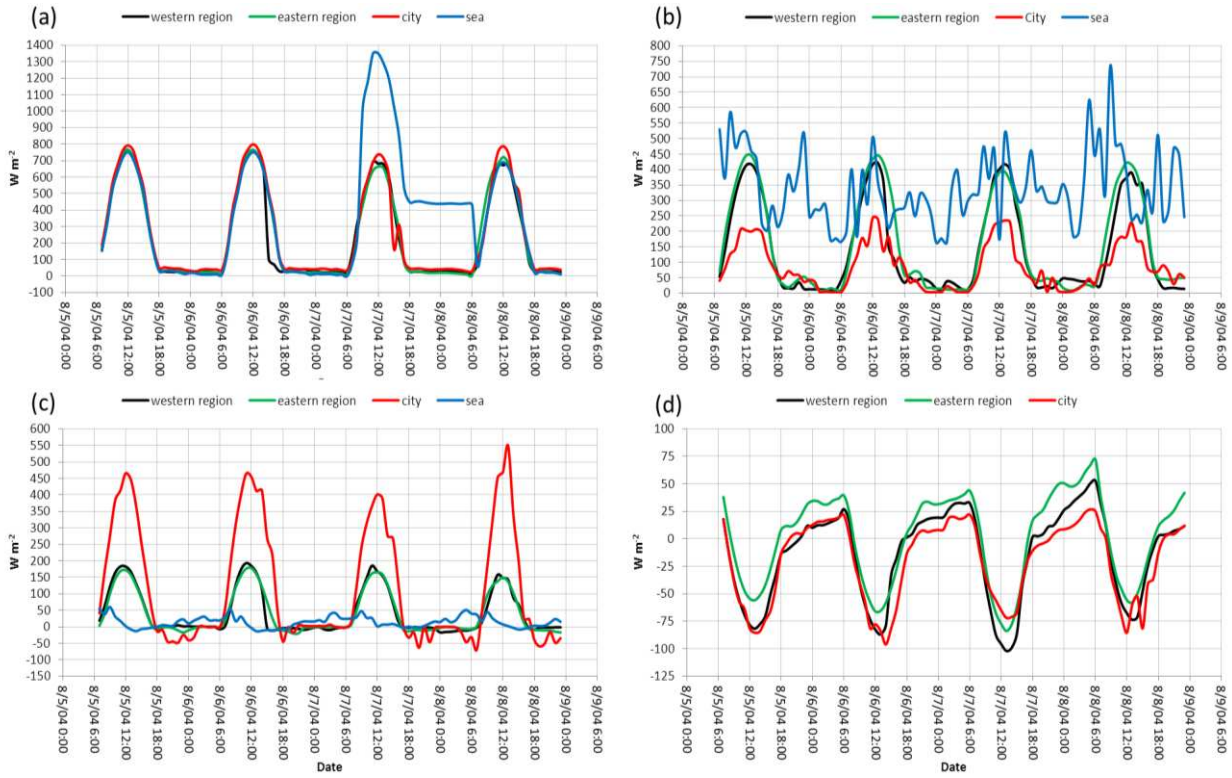

Figure 4. Simulated (a) incoming SWR, (b) outgoing SWR, (c) incoming LWR, and (d) outgoing LWR at the surface (Wm^{-2}) over JNR.

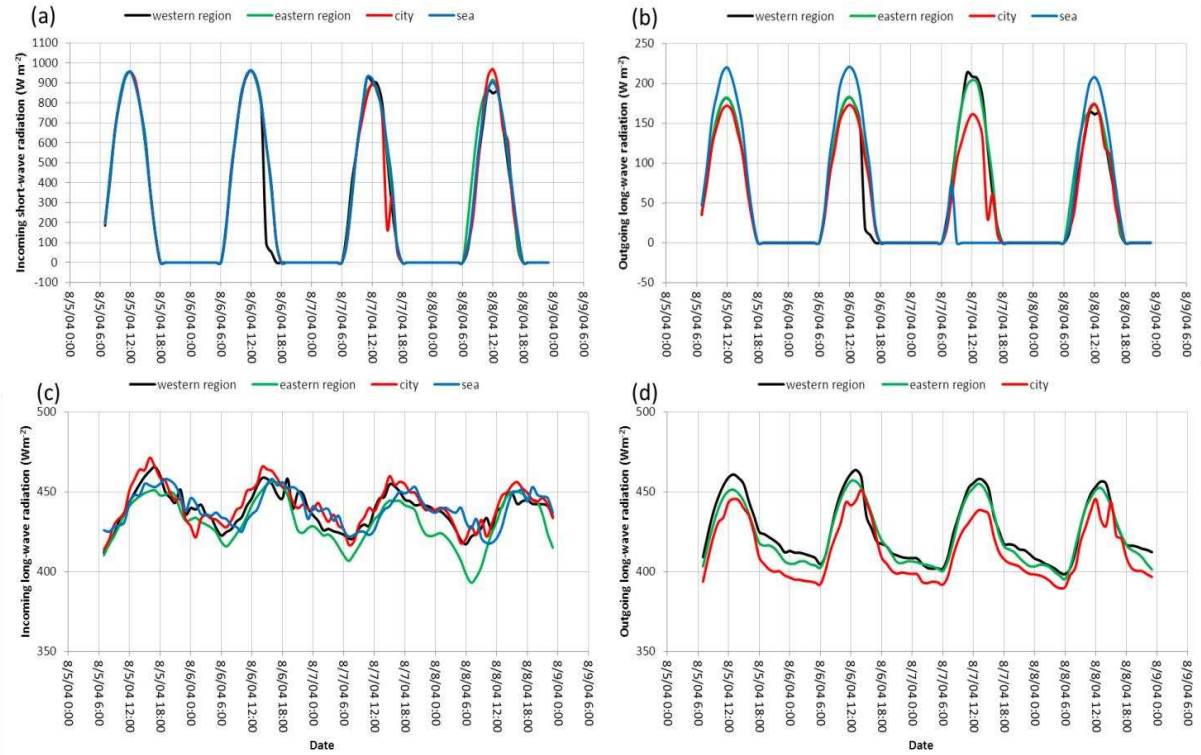

Figure 3. Simulated (a) SEB, (b) sensible heat, (c) latent heat, and (d) ground heat at the surface (Wm-2) over JNR.

Figure 5a shows SEB obtained from modified land cover MM5 model and how energy is allocated at difference places. It is shown that SEB is higher in the city in the daytime. The maximum net radiations of 800 Wm^{-2} and 780 Wm^{-2} are found in the daytime on August 06 and 07, respectively. The condition can be explained because less energy is lost; the energy is exchanged into sensible heat and lead to extra heat transfer to the air. In contrast to the western and eastern region because less sensible heat transfer occurs, energy is allocated more to evaporate water from vegetation and soil. Meanwhile in the nighttime, the sensible heat is negative and due to less evaporation, it leads the ground heat flux to play a dominant role in upward heat transfer to the atmosphere and keep balancing the energy in the city, western to eastern regions, and the sea. However, on August 07, the net radiation received at the sea area was more than 1,000 Wm^{-2}. Higher SEB occured in the day and nighttime. It can be explained that sensible heat is lower than latent heat. Thus, all energy is allocated to perform latent heat transfer in the daytime. Meanwhile, in the nighttime, the release of energy stored in the subsurface during daytime keep balancing higher energy at the sea in the nighttime and leads the surface temperature to be warmer. Simulation for each SEB components in eq. (2) are shown in Figure 5b, 5c, and 5d. It is noted that ocean ground heat flux is not calculated. In conclusion, high amount of energy is found in the tropical region during dry season. It would be best if SEB derived from the model is tested with the observation data, which is not available in the research. The boundary layer is also higher in the city. Meanwhile western region dominated by suburban showed higher boundary layer instead of eastern region (Figure 6a).

Figure 6d shows the simulation of surface sensible heat. It is shown that sensible heat is higher in the city area than surrounding regions. The positive sensible heat ranging between 350-500 Wm^{-2} occurs in the entire city. It is implied that higher sensible heat defines higher temperature at the same time. In addition, the observed sensible heat in the city and sea show much higher differences. Principally, the differences of sensible heat play major role in circulating the sea-breeze. Figure 6c shows simulated surface latent heat. As already mentioned that latent heat at the sea is much higher reaching 550 Wm^{-2} in the northeast and much lower in the northwest reaching 250 Wm^{-2}. The reason for this is that water released from the air to the surface and most of the energy is exchanged to the sensible heat causing higher temperature in the northwestern of the Java Sea. As shown in figure 6c that higher temperature then moves to the city and increase city's surface temperature. The latent heat is higher in the agricultural region. The energy of 450 Wm^{-2} is distributed over the east and southeast region since tea plantation and other organic farming are cultivated there. Meanwhile, the energy of 550 Wm^{-2} is distributed in rural area border the city in the west since the only well-growth crops during dry season are planted there.

Figure 6c and 6d show that high differences of surface latent and sensible heat fluxes occurs between city and west region. Thus, it might have led to a strong development of horizontal gradient. As a result, urban thermal will circulate to the west, accompanied by slowly increase of local temperature and reach the strongest effect of urban heat island at night (Ilhamsyah, 2012), as shown in Figure 6e and Figure 6f.

Bowen Ratio (BR) describing the ratio of surface sensible and latent heat fluxes over the city and its surrounding areas are depicted in figure 6b. Irrigated cropland and pasture characterized in both western and eastern areas show that during daytime from 7.00 LST – 13.00 LST, BR range from 0.2-0.5 which is typically values over irrigated crops and grassland, the positive sensible heat and latent heat have slight differences even though latent heat is dominant in the rural areas. Meanwhile after 15.00 LST and during nighttime, BR values are much lower which are less than 0. It can be explained that in the afternoon and during nighttime, negative sensible heat is developed since the surface is cooler than the air above and latent heat is higher to conduct a radiative cooling at night therefore it may result in negative values of BR. In addition, BR observed over the Sea are higher in the morning and lower in the afternoon, and during nighttime, it increase and reach 0.1 at midnight. Because of much higher differences of values observed between sensible and latent heat, therefore the fraction of these two variables may result in small number of BR. However, at the

sea, positive sensible heat flux occurred at night reflecting that heat is stored (negative sensible heat) during daytime and higher latent heat transfer occurred over the time.

The interesting variations of BR occurred over the city representing the urban and built-up land. During daytime, BR fluctuate from 1.5 – 3 and suddenly decrease to -0.5 in late afternoon. The fluctuation of BR are still observed at night until it reaches 0.75 at midnight and start decreasing gradually afterwards. The decreasing values of BR in late afternoon and early evening are due to negative sensible heat. However, as a result of the urban heat island effect, the positive sensible heat is developed once again and lead to the increase of BR at night as observed on August 06. However, in the next evening, the negative sensible heat is developed and less heat is lost due to evaporation, it then results in small number of BR.

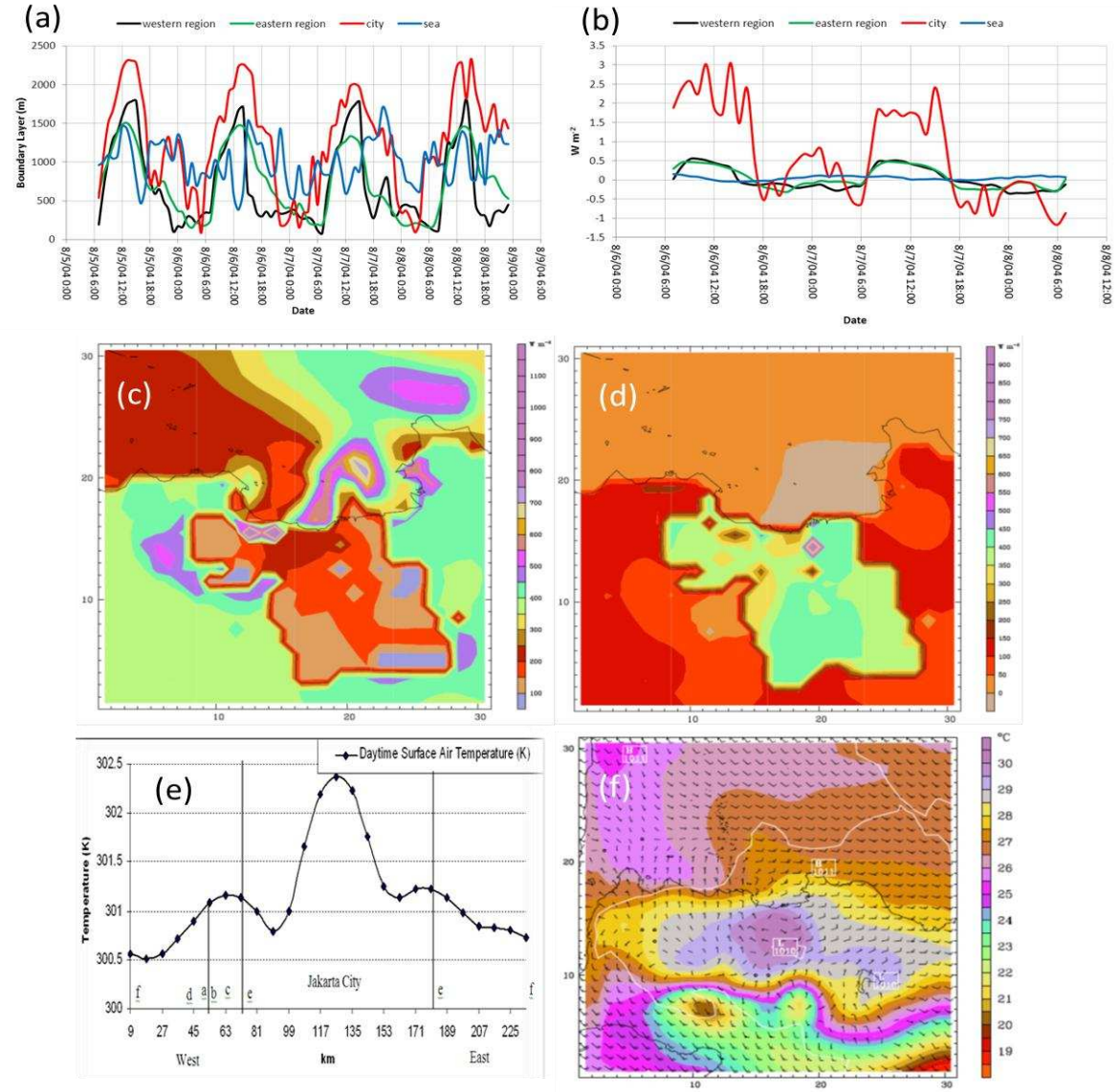

Figure 5. Simulated (a) boundary layer (m), (b) BR, (c) and (d) surface latent and sensible heat fluxes in the afternoon on August 08, (e) and (f) west-east section and spatial location of urban heat island on August 06 in the afternoon.

Conclusions

MM5 with specified physical schemes and modified land cover give a good result even though slight differences in achieving the peak of maximum temperature are found when it is compared with those of observation. The simulated SEB representing gain and loss of heat due to sensible, latent and ground heat is well-justified. During day and nighttime on August 6, heat loss in the city is less due to higher positive sensible heat flux in the city. The energy received at the surface is different between city and western-eastern regions. The variation is highly influenced by local weather formation which might be affected by cloud cover or other related-meteorological conditions. The condition, then, determine the amount of energy received at the surface. On the other hand, physical properties such as albedo, soil moisture, thermal properties also affect the variation of the energy received at the surface. SEB is higher in the city instead of west and east region reaching 800 Wm^{-2} in the daytime. The condition is due to higher energy exchanges causing more heat transfer to the atmosphere. On the contrary, heat transfer is less in the western and eastern region since most of the energy is allocated to evaporate water from soil and vegetation in those regions. BR representing the land cover characteristics is well-reflected. BR 0.1, 0.2, 0.5 and 3 over the sea, irrigated cropland, grassland and the urban built-up land are well-observed even though some variation may occur during day and nighttime due to air temperature, and specific land cover characteristics, e.g. albedo, soil moisture, emissivity, surface roughness and thermal inertia.

References

Aquilina, N., Dudek, A.V., Carvalho, A., Borrego, C. and Nordeng, T.E. (2005). MM5 high resolution simulations over Lisbon. Geophysical Research Abstracts, 7: 08685.

Brazel, A., Grossman-Clarke, S., Zehnder, J.A. and Hedquist, B.C. (2003). Observations and MM5 simulations of the urban heat island in Phoenix, Arizona, USA with a modified land cover scheme. Proceedings of fifth international conference on urban climate. Lodz, Poland September 1-5, 2003. Available at: http://nargeo.geo.uni.lodz.pl/~icuc5/text/O_8_3.pdf . (Accessed on 1 April 2008).

Dagestad, K.F., Johannessen, J., Hauge, G., Kerbaol, V. and Collard, F. (2006). High-resolution wind field retrievals off the Norwegian Coast: comparing ASAR observations and MM5 simulations. Proceedings of OceanSAR 2006 – Third Workshop on Coastal and Marine Applications of SAR. St. John's, Canada October 2006.

Deng, A. and Stauffer, D.R. (2006). On improving 4-km mesoscale model simulations. Journal of Applied Meteorology and Climatology, 45: 361-381.

Dudhia, J. (1993). A non-hydrostatic version of the Penn State – NCAR mesoscale model: validation tests and simulation of an Atlantic cyclone and cold front. Monthly Weather Review, 121: 1493-1513.

Durante, F. and de Paus, T. (2006). A comparison of MM5 and Meteo mast wind profiles at Cabauw the Netherlands and Wilhelmshaven Germany. e-WindEng, 3: 1-7.

Grossman-Clarke, S., Zehnder, J.A., Stefanov, W.L., Liu, Y. and Zoldak, M.A. (2005). Urban modification in a mesoscale meteorological model and the effects on near-surface variables in an arid metropolitan region. Journal of Applied Meteorology and Climatology, 44: 1281-1296.

Grossman-Clarke, S., Liu, Y., Zehnder, J.A. and Fast, J.D. (2007). Simulation of the urban planetary boundary layer in an arid metropolitan area. Journal of Applied Meteorology and Climatology, 47: 752-768.

Holtslag, B. and Steeneveld, G.J., (2008). Mesoscale meteorological modeling (MAQ-31806). Wageningen University, The Netherland.

Ilhamsyah, Y. (2012). A mesoscale meteorological model of modified land cover to the effect of urban heat island in Jakarta. Aceh International Journal of Sciences and Technology, 1(2): 60-66.

Oncley, S.P. and Dudhia, J. (1995). Evaluation of surface fluxes from MM5 using observations. Monthly Weather Review, 123: 3344-3357.

Pielke, R.A., Sr. (2002). Mesoscale meteorological modeling, 2nd Edition. Academic Press, San Diego, USA.

Rouse, W.R., Oswald, C.M., Binyamin, J., Blanken, P.D., Schertzer, W.M. and Spence, C. (2003). Interannual and seasonal variability of the surface energy balance and temperature of central great slave lake. Journal of Hydrometeorology, 4: 720-730.

Ruiz-Arias, J.A., Pozo-Vázquez, D., Sánchez-Sánchez, N., Montávez, J.P., Hayas-Barru, A. and Tovar-Pescador, J. (2008). Evaluation of two MM5-PBL parameterizations for solar radiation and temperature estimation in the South-Eastern area of the Iberian Peninsula. Il Nuovo Cimento, 31C(5-6): 825-842.

Sindosi, O.A., Bartzokas, A., Kotroni, V. and Lagouvardos, K. (2012). Verification of precipitation forecasts of MM5 model over Epirus, NW Greece, for various convective parameterization schemes. Natural Hazards and Earth System Sciences, 12: 1393–1405.

Sofyan, A., Kitada, T. and Kurata, G. (2005). Characteristics of local flow in Jakarta, Indonesia and its implication in air pollution transport. Proceedings of Atmospheric Sciences and Air Quality Conference. San Francisco, California April 27-29, 2005. Available at: ams.confex.com/ams/pdfpapers/90815.pdf (Accessed on 15 April 2008).

Sofyan, A., Kitada, T. and Kurata, G. (2007). Difference of sea breeze in Jakarta between dry and wet Seasons: implication in NO2 and SO2 distributions in Jakarta. Journal of Global Environment Engineering, 12: 63-85.

Stull, R.B. (2000). Meteorology for scientists and engineers, 2nd edition. Brooks/Cole, Thomson Learning, USA.

Su, Z. (2002). The Surface Energy Balance System (SEBS) for estimation of turbulent heat fluxes. Hydrology and Earth System Sciences, 6(1): 85-99.

Tokairin, T., Sofyan, A. and Kitada, T. (2009). Numerical study on temperature variation in the Jakarta area due to urbanization. Proceedings of the seventh International Conference on Urban Climate. Yokohama, Japan June 29 – July 3, 2009.

Trenberth, K.E. (2014). Energy and Climate. Available at: http://www.rmets.org/weather-and-climate/climate/energy-and-climate-dr-kevin-e-trenberth? Accessed on March 3, 2014.

Xin, X. and Liu, Q. (2010). The two-layer surface energy balance parameterization scheme (TSEBPS) for estimation of land surface heat fluxes. Hydrology and Earth System Sciences, 14: 491-504.